THE JOURNAL OF BIOLOGICAL CHEMISTRY
Vol. 277, No. 13, Issue of March 29, pp. 11385–11391, 2002
Printed in U.S.A.

The Structural Basis for the Specificity of Retinoid-X Receptor-selective Agonists: New Insights Into the Role of Helix H12*

Received for publication, November 13, 2001, and in revised form, December 19, 2001
Published, JBC Papers in Press, January 8, 2002, DOI 10.1074/jbc.M110869200

James D. Love‡§, John T. Gooch‡, Szilvia Benko¶, Chuan Li‖, Laszlo Nagy¶, V. Krishna K. Chatterjee§, Ronald M. Evans‖‡‡, and John W. R. Schwabe‡‖§§**

From the ‡Medical Research Council, Laboratory of Molecular Biology, Cambridge CB2 2QH and the §Department of Medicine, University of Cambridge, Addenbrooke's Hospital, Cambridge CB2 2QQ, United Kingdom, the ¶Department of Biochemistry and Molecular Biology, University of Debrecen, Medical and Health Science Center, Nagyerdei krt. 98, Debrecen H-4012, Hungary, and the ‡‡Howard Hughes Medical Institute and the ‖Salk Institute for Biological Studies, Gene Expression Laboratory, La Jolla, California 92037

Ligands that specifically target retinoid-X receptors (RXRs) are emerging as potentially powerful therapies for cancer, diabetes, and the lowering of circulatory cholesterol. To date, RXR has only been crystallized in the absence of ligand or with the promiscuous ligand 9-cis retinoic acid, which also activates retinoic acid receptors. Here we present the structure of hRXRβ in complex with the RXR-specific agonist LG100268 (LG268). The structure clearly reveals why LG268 is specific for the RXR ligand binding pocket and will not activate retinoic acid receptors. Intriguingly, in the crystals, the C-terminal "activation" helix (AF-2/helix H12) is trapped in a novel position not seen in other nuclear receptor structures such that it does not cap the ligand binding cavity. Mammalian two-hybrid assays indicate that LG268 is unable to release co-repressors from RXR unless co-activators are also present. Together these findings suggest that RXR ligands may be inefficient at repositioning helix H12.

The retinoid-X receptors (RXRα, β, and γ)[1] are nuclear receptors that regulate differentiation, development, and homeostasis in response to ligand (1–5). RXRs can act as either homodimers or heterodimers with other nuclear receptors (1, 6–8). The ability to serve as the preferred heterodimeric partner of many (>10) other receptors makes RXRs unique within the family of nuclear receptors and accounts for their role in many diverse signaling pathways. It is generally held that 9-cis retinoic acid (9cRA) is the natural ligand for RXRs (9, 10). This is a promiscuous ligand because it also activates retinoic acid receptors (RARs), which themselves serve as heterodimeric partners for RXR. Chemical approaches have led to the development of synthetic agonists that allow RXR to be activated without influencing the activity of RARs (11, 12). It has emerged that RXR-specific agonists such as Targretin® and LG268 may serve as beneficial therapies for the treatment of cancer, diabetes, and other metabolic disorders (13–15). LG268 is a substituted stilbene (6-[1-(3,5,5,8–8-pentamethyl-5,6,7,8-tetrahydronapthalen-2-yl)-cycloproyl]-nicotinic acid) that specifically binds to and activates RXRs, but not RARs, with a slightly higher affinity than 9cRA (9–11).

Structural and biochemical studies of a number of nuclear receptor ligand-binding domains (LBDs) have yielded a relatively simple model for the mechanism by which ligands regulate nuclear receptor activity. The LBDs of nuclear receptors share a common, predominantly helical fold (16, 17). In the absence of ligand, co-repressor proteins bind to the surface of the LBD and prevent the C-terminal helix H12 (AF2-helix) from binding to the surface of the receptor (18–20). Activating ligands bind in a hydrophobic cavity within the core of the LBD and cause the repositioning of helix H12 such that it seals the ligand binding cavity, resulting in the displacement of co-repressor. In this position, helix H12 forms a critical part of the binding site for co-activator proteins (21, 22). Significantly, ligands that do not activate nuclear receptors (competitive antagonists) appear to exert their effect by displacing helix H12 from its "active position" so that it occupies the co-activator binding site, the so-called antagonist conformation, and thus prevents co-activator binding (23, 24). Furthermore ligands that act as partial agonists have been found to cause helix H12 to adopt a similar position to that seen with full antagonists (25).

Here we present the first structure of RXR bound to a selective agonist, LG268. This structure shows clearly why LG268 will bind only to RXR and not to RARs. It also suggests why LG268 has a somewhat higher affinity for RXR than does 9cRA and why it is a more potent agonist. The liganded RXR forms a stable homodimer with the interface very similar to that of the apo-homodimer (26, 27). Finally, helix H12 adopts a novel position not seen in other liganded nuclear receptors. Although this position may be favored in the crystal lattice, it suggests that helix H12 is only weakly recruited to the canonical active position on binding ligands. Support for this comes from mammalian two-hybrid experiments showing that, unlike with other receptors, both ligand and co-activator are required to

* The work was supported in part by the Royal Society International Exchange Program and the European Union FP5. The costs of publication of this article were defrayed in part by the payment of page charges. This article must therefore be hereby marked "*advertisement*" in accordance with 18 U.S.C. Section 1734 solely to indicate this fact.

The atomic coordinates and structure factors (code 1h9u) have been deposited in the Protein Data Bank, Research Collaboratory for Structural Bioinformatics, Rutgers University, New Brunswick, NJ (http://www.rcsb.org/).

** Recipient of the Boehringer Ingelheim Research Award, an International Scholar of the Howard Hughes Medical Institute, and an EMBO young investigator.

§§ To whom correspondence should be addressed: MRC-Laboratory of Molecular Biology, Hills Rd., Cambridge CB2 2QH, UK. Tel.: +44-1223-402064; Fax: +44-1223-213556; E-mail: John.Schwabe@mrc-lmb.cam.ac.uk.

[1] The abbreviations used are: RXR, retinoid-X receptor; 9cRA, 9-cis retinoic acid; LBD, ligand-binding domain; RAR, retinoic acid receptor; atRA, all-trans retinoic acid; TR, thyroid hormone receptor; VP, VP16 activation domain; Gal, Gal4 DNA-binding domain; SMRT, silencing mediator for retinoid and thyroid hormone receptors; ACTR, activator for thyroid and retinoid hormone receptors; ESRF, European Synchrotron Radiation Facility.

TABLE I
Data collection, processing, and refinement statistics
$R_{merge} = \Sigma|I - \langle I\rangle|/\Sigma\langle I\rangle$; R_{cryst} and $R_{free} = \Sigma|F_{obs} - F_{calc}|/\Sigma F_{obs}$. RMSD, root-mean-square deviations from ideal values.

X-ray source/wavelength	ESRF ID14–2/0.933Å
Resolution (outer shell)	38–2.7 (2.87–2.7) Å
Total/unique reflections	87647/29713
Redundancy/completeness	2.9/97.8%
R_{merge} (outer shell)	9.8% (26.4%)
I/σ (outer shell)	5.1 (2.1)
Space group	C2, a = 123.89, b = 106.88, c = 100.59, β = 122.56
R_{cryst}/R_{free} *(10%)*	27.7/30.1%
RMSD bonds/angles	0.009Å/1.4°
Average B-factor	51.0 Å^3
Ramachandran	
Favored/additional/generous	91.8/8.2/0.0%

displace co-repressor and hence suggesting that co-activator helps to stabilize the helix in the active conformation.

EXPERIMENTAL PROCEDURES

Expression, Purification, and Crystallization—The ligand-binding domain of hRXRβ (amino acids 296–533) was over-expressed in *Escherichia coli* (BL21(DE3)) and purified as a stoichiometric heterodimer with hRARβ as described previously (28). The pure protein, in a buffer containing 10 mM Tris-HCl, pH 8.0, 50 mM NaCl, 1.0 mM dithiothreitol, and 0.125% (v/v) Triton X-100, was incubated for 16 h with LG268 and TTNPB at a 1.2 molar excess and subsequently concentrated to 7.4 mg/ml using a Centricon concentrator (Amicon). Ligands dissolved in Me_2SO were diluted in the protein solution such that the final Me_2SO concentration was <1%.

Crystals were grown at 20 °C using the vapor diffusion method. 2-μl drops were equilibrated against 1.4 M ammonium formate, pH 7.6. Irregular plate crystals (~400 × 300 × 20 μm) formed after 3 months in a bed of precipitate that was found to be denatured hRARβ LBD. Small crystals of the hRXRβ LBD (expressed without the hRARβ LBD) could be grown under similar conditions but without detergent, suggesting that the detergent plays a role in dissociating the heterodimer but not in the crystallization itself. Crystals were harvested using a 400-μm loop mounted on a pin and frozen by being plunged into liquid nitrogen using the reservoir solution supplemented with 25% glycerol as a cryoprotectant. Analysis of the crystals suggested that the hRXRβ LBD had not been proteolyzed during crystallization.

Structure Solution and Refinement—X-ray diffraction data were collected at 100 K using a refrigerated nitrogen gas delivery system at beamline ID14–2 ESRF (Grenoble, France) on an area detector systems Quantum-4 CCD. Data were processed using Mosflm (29) and further using the CCP4 package (30). The best crystals diffracted beyond 2.5 Å with useful data to 2.7 Å. Data processing statistics are shown in Table I. The structure was solved by molecular replacement with a search model comprising a dimer, the apo-RXRα LBD (amino acids 225–431) lacking the C-terminal structural elements helices H11 and H12. Clear rotation and translation function solutions were obtained using CNS (15–4 Å) (31). The initial *R*-factor following rigid body refinement was 46.9%. The sigma-a weighted $2F_o - F_c$ map was substantially improved using NCS averaging and solvent flipping implemented in CNS. Strict NCS restraints were imposed followed by four rounds of rebuilding and refinement in O (32) and CNS, respectively. The NCS restraints were then released, and further refinement gave a final model for which statistics are shown in Table I.

Transient Transfection Experiments—Mammalian expression vectors used in this work have been described previously (18) with the exception of the ACTR vector, which was based on the pcDNA3.1 vector (Invitrogen) and contained the receptor interaction domain (amino acids 621–821) with an N-terminal nuclear localization signal from SV40. CV1 cells were transiently transfected as described previously (18). Luciferase activity for each sample was normalized with reference to the level of β-galactosidase activity of a control reporter construct. Each transfection was carried out in triplicate at least three times.

RESULTS

Structure Determination—hRXRβ:LG268 crystallized in space group C2 with two LBD dimers in the asymmetric unit. The structure was solved by molecular replacement using a truncated version of the apo-hRXRα dimer as the search model (33). The structure of the apo-hRXRα was chosen as a starting model because it is the only available RXR homodimer structure and it would serve as an unbiased model from which to interpret the structural changes on binding ligand. An excellent electron density map was obtained by averaging according to the 4-fold noncrystallographic symmetry. The map showed clear electron density for the majority of the hRXRβ LBD and the bound ligand, LG268. However the extreme N and C termini of the LBD could not be assigned in the electron density map nor could an internal loop between helices H1 and H3 (amino acids 312–334).

Crystal Packing—The hRXRβ LBDs are packed in the crystal lattice as octamers (two asymmetric units) with each monomer making extensive contacts to two other LBDs (Fig. 1*a*). One of these two interfaces is clearly the biologically relevant homodimerization interface (marked *HDI*) with a buried surface of 2250 Å^2. The other interface, which buries 1660 Å^2, arises as part of the crystal packing (marked *CPI*). Additional electron density seen at this second interface could not be attributed to protein and is most likely either a partially ordered detergent molecule or an additional molecule of the ligand. Because of this ambiguity, no model was fitted to this density or included in the refinement.

Adjacent octamers pack together in the crystal lattice with a tightly bound metal ion at the interface (shown as *gray spheres*, Fig. 1*a*). This ion, chelated by His-402 and His-404 in one monomer and by Asp-390 in another, was assigned as a Ni^{2+} ion that was presumably retained during the purification on the nickel-nitrilotriacetic acid resin. There is clearly additional density for a fourth ligand for the Ni^{2+}, which was tentatively modeled as a chloride ion.

Overall Structure—The hRXRβ:LG268 structure has an overall architecture similar to that of LBDs from other members of the nuclear receptor family (16). To facilitate comparison with other structures, we used a secondary structure numbering scheme based on the original apo-hRXRα structure (33). The hRXRβ LBD consists of a three-layer helical sandwich (Fig. 1*b*). Helices H1 and H3 comprise one outer layer (joined by a disordered loop). The central layer comprising helices H4, H5, H8, and H9 is incomplete, leaving a cavity that accommodates bound ligand. The final layer comprises helices H7, H9, and H10/H11 and forms the homodimer interface between the two LBD monomers. The position of helix H12 in the hRXRβ:LG268 complex differs from that seen in previous RXR structures (Fig. 1, *c–e*). The significance of this difference is discussed further below.

Ligand Binding—The initial electron density map, averaged according to the noncrystallographic symmetry, showed unambiguous density for the LG268 ligand (Fig. 2*a*). It is enclosed in a largely hydrophobic cavity (568 Å^3) bounded by helices H3, H5, H7, and H11 and a β-sheet. The ligand (355 Å^3) occupies 63% of the cavity, making extensive contacts with the protein (Fig. 2*b*). The majority of contacts are nonpolar van der Waals interactions. However, the carboxylate of the nicotinic acid group forms a salt bridge with Arg-387 and accepts hydrogen bonds from the backbone amide of Ala-342 and an ordered water molecule. Ile-339, Leu-380, and Phe-384 contact the piperidine ring, and the cyclopropyl group is in close contact with Trp-376, Asn-377, and Ile-381. Significantly there is no hydrogen bonding partner for the nitrogen in the piperidine ring, and therefore the rotational orientation of the ring could not be assigned.

The naphthalene ring, with its five methyl substituents, makes the bulk of the van der Waals interactions with the protein and contacts 10 side chains within the ligand binding

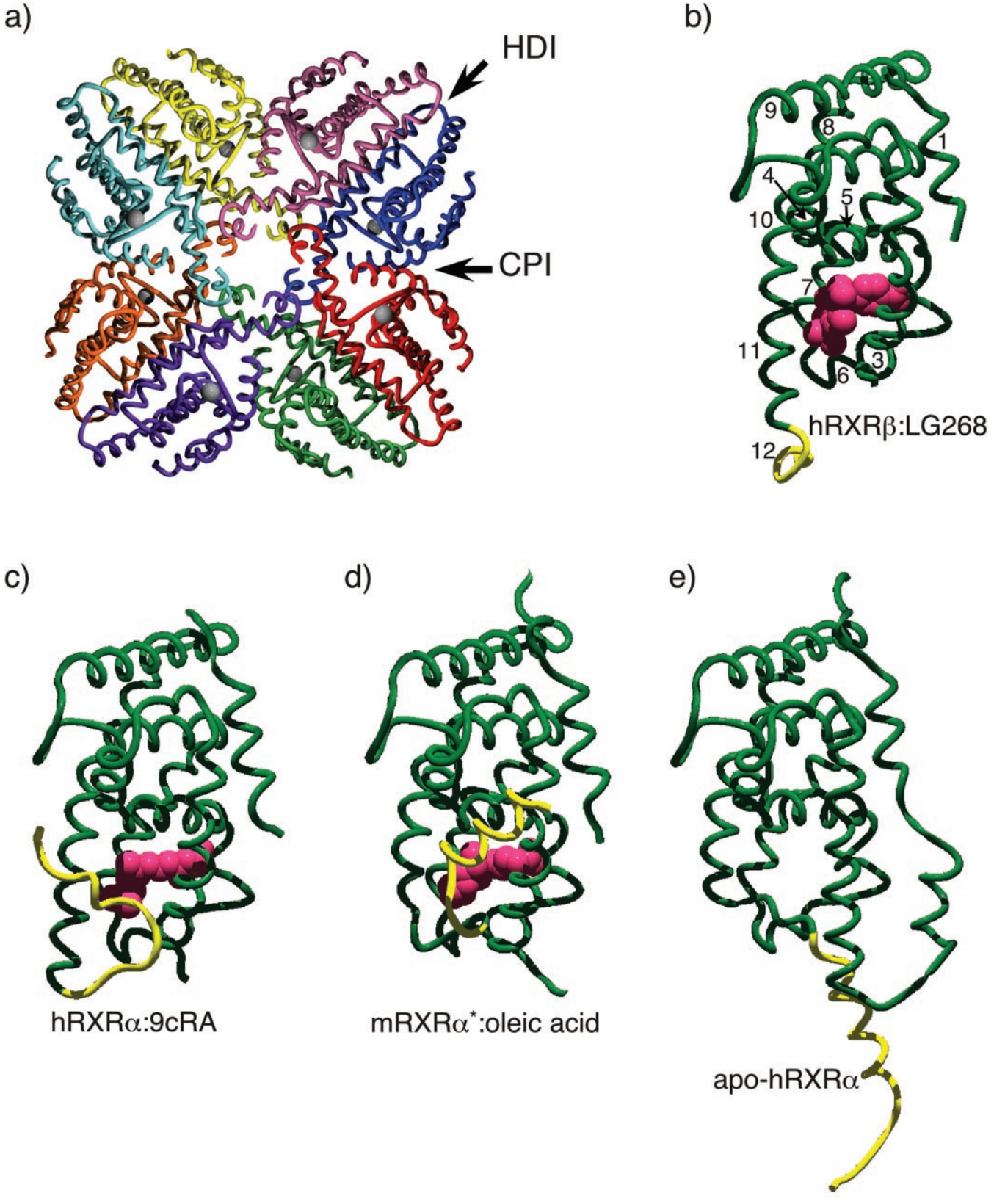

FIG. 1. **Comparison of hRXRβ:LG268 with hRXRα structures.** *a*, hRXRβ:LG268 packs within the crystal as a tetramer of homodimers. *HDI* and *CPI* indicate the homodimer and crystal packing interfaces, respectively. The *gray spheres* indicate nickel ions that are involved in interoctamer packing interactions. *b*, structure of hRXRβ:LG268. The helices that make up the three-layer antiparallel α-helical sandwich are shown in *green*. Helix H12 is shown in *yellow*, adopting a position reminiscent of the apo-hRXRα ligand-binding domain. *c–e*, structures of hRXRα showing the various orientations adopted by helix H12 (*yellow*). hRXRα:9cRA (38) (Protein Data Bank code 1fby), mRXRα*-oleic acid (36) (Protein Data Bank code 1dkf), and apo-hRXRα (33) (Protein Data Bank code 1lbd).

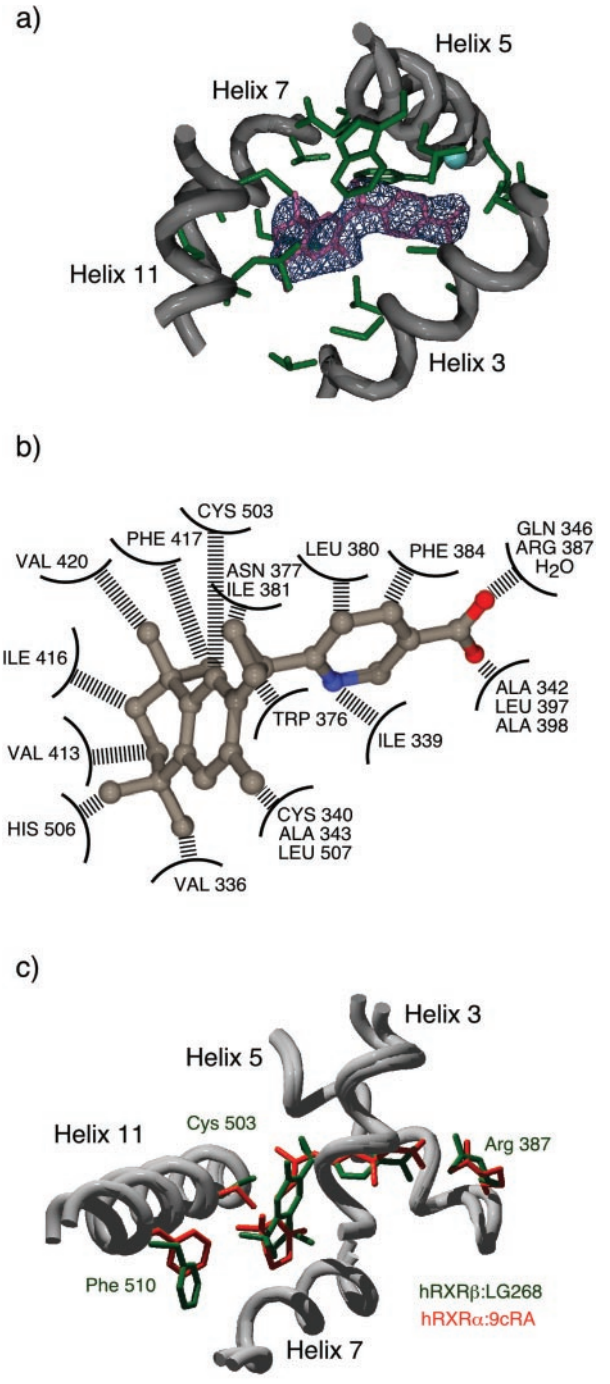

FIG. 2. **Contacts to LG268 and comparison with hRXRα:9cRA.** *a*, the ligand binding pocket of hRXRβ:LG268. The $2F_o - F_c$ electron density for the ligand is shown in *blue* (contoured at $\sigma = 1$). The electron density shown is prior to refinement but after averaging according to the 4-fold noncrystallographic symmetry and allows unambiguous placing of the ligand. Side chains that contact the ligand are shown in *green* (within 4.5 Å), and a water molecule is shown as a *blue sphere*. *b*, schematic representation of the contacts between the protein and the LG268 ligand. *c*, superposition of the ligand binding cavities of hRXRβ:LG268 (*green*) and hRXRα:9cRA (*red*) (38) (Protein Data Bank code 1fby). Side chains that reorientate to accommodate the different ligands are labeled.

cavity. The methyl on the unsaturated ring of the naphthalene makes van der Waals contacts to Cys-340, Ala-343, and Leu-507 and protrudes out from the ligand binding cavity toward the canonical position of helix H12. Comparison with other liganded RXR structures suggests that the methyl would be in close van der Waals contact with Leu-522 in helix H12 if it were in the canonical agonist position.

Comparison with hRXRα Bound to 9cRA—LG268 binds to all three RXR isoforms with a dissociation constant of ~3 nM (11); this contrasts with the somewhat weaker dissociation constant of 9cRA (9–12 nM for hRXRα) (9, 10). Notably, LG268 also gives 50% maximal activation at a concentration at least 10-fold lower than 9cRA (34).

The general pattern of the contacts between RXRβ and LG268 is very similar to that seen in the RXRα:9cRA structure. The similarity extends to the presence of an ordered water molecule in the ligand cavity and is unsurprising because both ligands are in van der Waals contacts with all of the side chains exposed in the interior of the ligand binding cavity (Fig. 2*b*). The only differences involve side chain rearrangements to accommodate the different shape of LG268. The most significant rearrangements are those of residues Cys-503, Phe-510, and Arg-387 (Fig. 2*c*). Notably, the orientation of Cys-503 seen in the hRXRα:9cRA structure is incompatible with LG268 binding, as it would result in a severe steric clash. Rotation about the Cα–Cβ bond allows the Cys-503 to accommodate LG268 binding, but in this new position it would clash with 9cRA. The movement of Cys-503 also requires the further rearrangement of the side chain of Ile-416.

Structural Basis for the Specificity of LG268—In contrast to the promiscuous properties of 9cRA, which also activates retinoic acid receptors (RARs), LG268 is highly specific for RXRs (the K_d for RARs is >1000 nM (11)). This raises the question as to why, unlike 9cRA, LG268 is unable to bind to and activate RARs. Fig. 3 shows a comparison of the hRARγ and hRXRβ ligand binding pockets. Superposition of the RXRβ and RARγ structures on helices H5 and H11 provides the most instructive comparison of the two structures. It is clear that the paths of helix H3, the β-sheet, as well as helices H6 and H7 adopt significantly different conformations relative to helices H5 and H11 and the rest of the structure (Fig. 3, *a* and *b*). These differences in secondary structure positioning, along with different side chain identities, result in a differently shaped ligand binding pocket (Fig. 3, *c* and *d*). In particular the side chains of residues Leu-268, Met-272, Phe-288, Phe-304, Gly-393, Arg-396, and Ala-397 in hRARγ combine to create a relatively linear cavity suited to accommodate the extended conformation of all-trans retinoic acid (atRA). The corresponding residues in hRXRβ (Asn-377, Ile-381, Leu-397, Val-413, Cys-503, His-506, and Leu-507) create a more globular cavity suited to accommodate a shorter "bent" ligand such as LG268 or 9cRA. Interestingly the side chain of Arg-387 is able to adjust its position so as to reach ~2 Å further into the ligand binding cavity to form a salt bridge with the carboxylate of LG268. These observations support the previous suggestion that it is the ability of 9cRA to flex that allows it to bind to both RARs and RXRs (35). The fact that LG268 is fixed in a bent conformation by the tetrahedral geometry around the cyclopropyl group means that it is unable to adopt the linear conformation needed to bind hRARγ and would therefore clash with the side chains of residues Phe-288, Phe-304, and Met-272. Similarly, atRA is fixed in a linear conformation and could not adapt to the shorter ligand binding cavity of RXR.

Homodimerization—In the structure of the hRXRβ bound to LG268, the receptor LBD forms a homodimer. The homodimerization interface is essentially identical to that observed in the apo-hRXRα dimer interface (27, 33). In previous crystals of liganded RXRs, the LBD was found to be either monomeric or bound as a heterodimer to a partner receptor (36–38). Because the apo-hRXRα was found to be a dimer or tetramer, it has been suggested that ligand binding favors dissociation of RXR

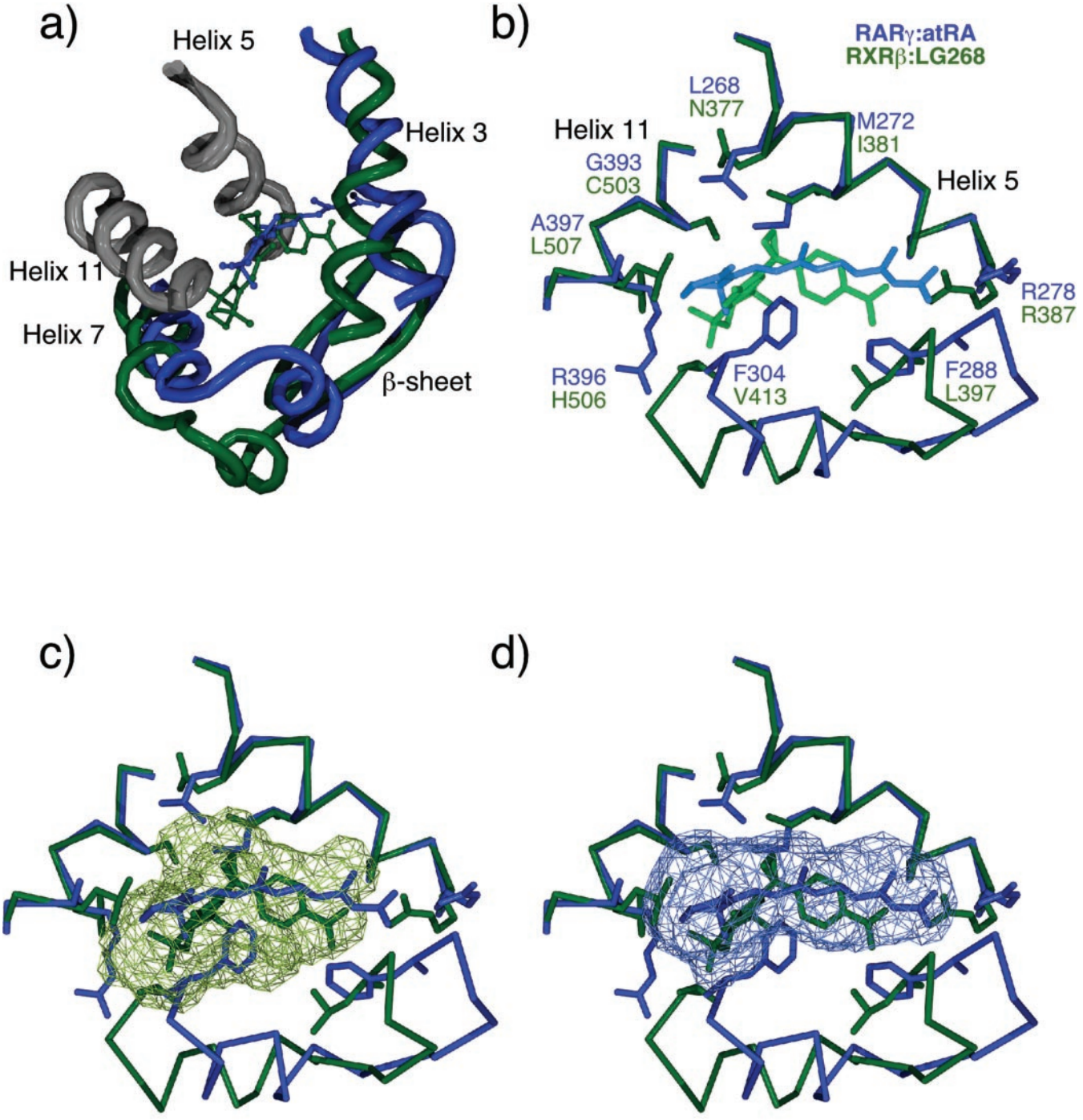

FIG. 3. **Comparison with hRARγ:atRA.** *a*, differences between hRXRβ:LG268 (*green*) and hRARγ:atRA (*blue*) (47) (Protein Data Bank code 2lbd) ligand binding pockets. The structures were superimposed using helices H5 and H11 (*gray*). Helices H3 and H7 and the β-sheet adopt largely different conformations in order to bind atRA. *b*, the critical amino acid residues that discriminate between RXR- and RAR-specific agonists. *c–d*, the shapes of the RXR (*green*) and RAR (*blue*) ligand-binding cavities. The cavity within RXR has a more globular shape in comparison with the more elongated RAR cavity.

oligomers and the formation of monomers or heterodimers (38, 39). However, a comparison with the hRXRα:9cRA structure suggests no obvious reason why it should be monomeric, whereas hRXRβ:LG268 (and indeed the apo-hRXRα) is a homodimer. It is therefore unclear how ligand binding might favor dissociation of the homodimer, and it seems likely that the hRXRα:9cRA crystal lattice favors the monomer.

A novel Position for Helix H12—As mentioned above, helix H12 adopts an unexpected orientation in the structure of hRXRβ bound to LG268. It is positioned such that it is folded under the ligand-binding domain and makes no contacts to the main body of the protein (Fig. 1*b*). Residues beyond Leu-522 are rather disordered. Because LG268 is a strongly activating ligand, we expected helix H12 to adopt the canonical active position. Accordingly, we examined the packing in the crystal lattice to determine whether it was compatible with the expected position of helix H12. It appears that for two adjacent proteins, one but not both could have helix H12 in the canonical position. Thus the crystal lattice precludes half of proteins from adopting the canonical position for helix H12. This raises the question: was helix H12 displaced from the expected position during crystallization or did the crystals select molecules in

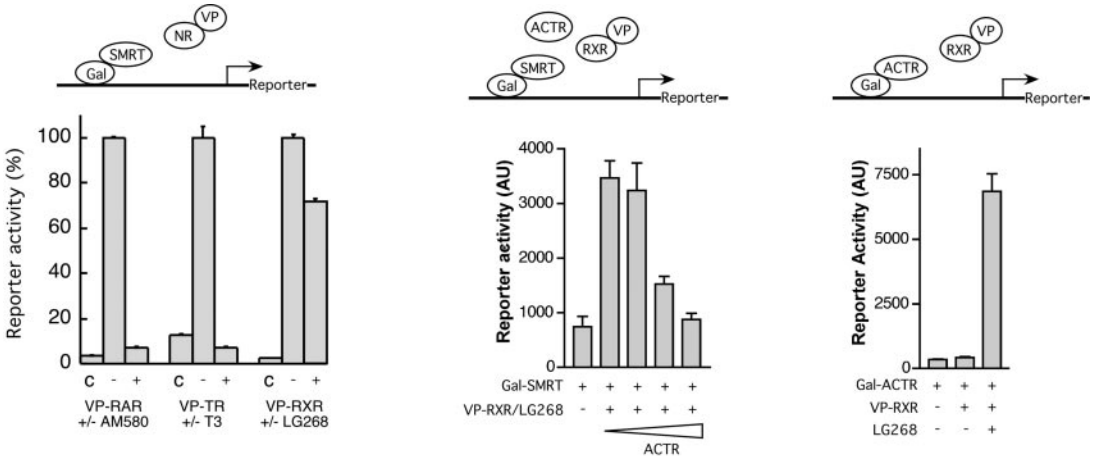

FIG. 4. **RXR ligands are inefficient at displacing co-repressor in the absence of co-activator.** Mammalian two-hybrid interaction assays indicate that unliganded receptors (TR, RAR, and RXR) all interact with the co-repressor protein SMRT. The addition of ligand results in dissociation of TR and RAR but not RXR (*left panel*). Increasing amounts of the co-activator ACTR, however, is able to displace co-repressor from RXR in the presence of ligand (*middle panel*). The *right-hand panel* shows the control experiment that ligand promotes co-activator interaction in the absence of co-repressor. Thus, ligand is absolutely required for the recruitment of co-activators but is insufficient to displace co-repressors from RXR.

which the helix was already elsewhere? In either situation it suggests that helix H12 is rather weakly recruited to the active position on binding ligand.

We and others (18–20, 40) have previously proposed that the repositioning of helix H12 is critical to the displacement of co-repressor proteins and the recruitment of co-activators. We have used mammalian two-hybrid assays to explore the role of LG268 in regulating co-factor interactions. These experiments show that, unlike other receptors such as TR and RAR, VP-RXR is efficiently recruited to the co-repressor hybrid Gal-SMRT even in the presence of ligand (Fig. 4). However, the addition of increasing amounts of the co-activator ACTR (fused to the SV40 nuclear localization signal) is able to compete for the VP-RXR such that interaction with Gal-SMRT is abolished. These results show that ligand alone is unable to reposition helix H12 and displace co-repressor. However in the presence of ligand, the co-activator is able to displace the co-repressor, resulting in an active complex. We propose that while RXR ligands are absolutely required for the recruitment of co-activators, they are insufficient to displace co-repressors unless co-activator is also present.

DISCUSSION

The application of synthetic chemistry techniques to the development of novel nuclear receptor ligands has proven extraordinarily powerful. It has been possible to derive receptor and isoform specific ligands, which do not occur in nature, as well as compounds with activities ranging from superactive agonists through to powerful antagonists. A remarkable feature of these synthetic ligands is that it is possible to generate a wide range of activities that depend upon their detailed chemistry rather than just their dissociation constants. This suggests that the activity of the receptor can be fine-tuned across a broad range of activity.

The retinoid-X receptor is an important therapeutic target for synthetic agonists because it is involved in a wide range of biological processes. Potential applications include the treatment of cancer and diabetes and the lowering of circulatory cholesterol.

To understand the structural and chemical bases for the specificity, 3–4-fold higher affinity, and >10-fold greater transactivation activity of LG268 compared with 9cRA, we crystallized the ligand with the human RXRβ ligand-binding domain. The structure reveals that several factors are likely to contribute to the greater affinity of LG268 for RXR. First, the synthetic ligand has a 13% larger volume than 9cRA (355 *versus* 315 Å^3) and thus occupies a greater fraction of the ligand-binding cavity (63% *versus* 57%) and has a correspondingly greater surface area of contact with the protein. Second, compared with 9cRA, LG268 is comparatively rigid such that the only free movement is the rotation of the naphthalene and piperidine rings. LG268 binding is therefore likely to be entropically favored compared with 9cRA. Indeed the geometry and volume of the cyclopropyl group would appear to be critical for the high binding affinity. The angle between the piperidine and naphthalene groups is fixed at <109°. If the cyclopropyl group is replaced with a smaller trigonal carbonyl or alkene group, the affinity is reduced then by >10-fold (11).

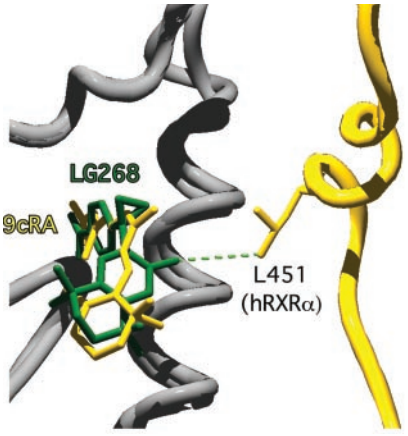

FIG. 5. **Potential contacts between LG268 and helix H12.** Superimposition of hRXRβ:LG268 (*green*) and hRXRα:9cRA:CoA (*yellow*) (37) (Protein Data Bank code 1fm6). Note that 9cRA makes no contact with residues in helix H12. LG268, however, is able to contact a leucine side chain in helix H12 via the methyl substituent on the unsaturated ring of the naphthalene. It is likely that in the LG268 complex this contact stabilizes helix H12 and facilitates co-activator binding compared with 9cRA. This may explain the significantly higher transcriptional activation by LG268 compared with 9cRA (some helices were removed for clarity).

Interestingly the increased transactivation activity of LG268 compared with 9cRA is proportionally greater than the increased binding affinity; which suggests that there is a secondary mechanism for this enhancement. A comparison of the

structure with that of hRXRα:9cRA:co-activator (37) (Fig. 5) indicates that unlike 9cRA, LG268 can make a direct contact with a leucine in helix H12. This contact is mediated by the methyl substituent on the unsaturated ring of the naphthalene. Thus LG268, but not 9cRA, is able to directly stabilize helix H12 and its interaction with co-activator. When a more bulky group occupies this position, the ligand acts as an antagonist, as demonstrated by the compound LG100754 (41, 42).

The C-terminal helix H12 of nuclear receptors plays a critical role in regulating the receptor. Receptors that lack helix H12 are unable to release co-repressors even in the presence of agonists and are equally unable to recruit co-activators (43–45). These observations fit well with our understanding of nuclear receptor structures. In its active conformation, helix H12 makes direct contacts with the coactivator helix and, in many receptors, with the ligand itself. Mutations that disturb that active position of helix H12 result in a loss of transactivation activity because of the inability to recruit coactivator (46). In the absence of ligand it has been proposed that helix H12 is displaced by co-repressor and so must adopt an alternate position or positions (18–20, 40). In a variety of unliganded antagonist and partial agonist bound structures, helix H12 has been seen to occupy a range of alternate positions. These observations suggest that helix H12 may exist in an equilibrium between various conformations. The position of the helix H12 equilibrium is likely to depend upon the nature of the ligand bound to the receptor.

We have shown that in the structure of hRXRβ bound to the synthetic agonist LG268, helix H12 does not adopt the active conformation. This may be a consequence of the packing in the crystal lattice trapping a particular position of helix H12. However, two lines of evidence suggest that the helix H12 position seen in the crystal may be indicative of the behavior of helix H12 *in vivo*. First, helix H12 of RXR is equally sensitive to proteolytic cleavage both in the presence and absence of ligand (44). This contrasts with other receptors, such as TR, and suggests that the accessibility of helix H12 in RXR is not influenced greatly by ligand and therefore that ligand may only weakly recruit helix H12 to the active conformation. Second, mammalian two-hybrid experiments suggest that efficient displacement of co-repressor by helix H12 requires the presence of both ligand and co-activator. We conclude from these observations that helix H12 in RXR is likely to be more mobile and less influenced by ligand alone than in certain other nuclear receptors. Indeed, the differences in the mobility of helix H12 among different receptors and receptor-ligand complexes are likely to underlie the widely diverse behavior of different receptors and ligands.

Acknowledgments—We thank the following persons for their help, advice, and encouragement: Ester Banayo, Pat Edwards, Louise Fairall, Heather Owen, and Adam Price. We are also grateful to the staff of the ESRF beamline ID14-2.

REFERENCES

1. Solomin, L., Johansson, C., Zetterstrom, R., Bissonnette, R., Heyman, R., Olson, L., Lendahl, U., Frisen, J., and Perlmann, T. (1998) *Nature* **395,** 398–402
2. Krezel, W., Ghyselinck, N., Samad, T. A., Dupe, V., Kastner, P., Borrelli, E., and Chambon, P. (1998) *Science* **279,** 863–867
3. Kastner, P., Mark, M., Leid, M., Gansmuller, A., Chin, W., Grondona, J. M., Decimo, D., Krezel, W., Dierich, A., and Chambon, P. (1996) *Genes Dev.* **10,** 80–92
4. Yu, V., Delsert, C., Andersen, B., Holloway, J., Devary, O., Naar, A., Kim, S., Boutin, J., Glass, C., and Rosenfeld, M. (1991) *Cell* **67,** 1251–1266
5. Mangelsdorf, D. J., and Evans, R. M. (1995) *Cell* **83,** 841–850
6. Forman, B., Umesono, K., Chen, J., and Evans, R. (1995) *Cell* **81,** 541–550
7. Kliewer, S. A., Umesono, K., Mangelsdorf, D. J., and Evans, R. M. (1992) *Nature* **355,** 446–449
8. Zhang, X., Hoffmann, B., Tran, P., Graupner, G., and Pfahl, M. (1992) *Nature* **355,** 441–446
9. Heyman, R. A., Mangelsdorf, D. J., Dyck, J. A., Stein, R. B., Eichele, G., Evans, R. M., and Thaller, C. (1992) *Cell* **68,** 397–406
10. Levin, A. A., Sturzenbecker, L. J., Kazmer, S., Bosakowski, T., Huselton, C., Allenby, G., Speck, J., Kratzeisen, C., Rosenberger, M., Lovey, A., and Grippo, J. F. (1992) *Nature* **355,** 359–361
11. Boehm, M., Zhang, L., Zhi, L., McClurg, M., Berger, E., Wagoner, M., Mais, D., Suto, C., Davies, J., Heyman, R., and Nadzan, A. M. (1995) *J. Med. Chem.* **38,** 3146–3155
12. Lehmann, J. M., Jong, L., Fanjul, A., Cameron, J. F., Lu, X. P., Haefner, P., Dawson, M. I., and Pfahl, M. (1992) *Science* **258,** 1944–1946
13. Gottardis, M. M., Bischoff, E. D., Shirley, M. A., Wagoner, M. A., Lamph, W. W., and Heyman, R. A. (1996) *Cancer Res.* **56,** 5566–5570
14. Mukherjee, R., Davies, P., Crombie, D., Bischoff, E., Cesario, R., Jow, L., Hamann, L., Boehm, M., Mondon, C., Nadzan, A., Paterniti, J., Jr., and Heyman, R. (1997) *Nature* **386,** 407–410
15. Miller, V. A., Benedetti, F. M., Rigas, J. R., Verret, A. L., Pfister, D. G., Straus, D., Kris, M. G., Crisp, M., Heyman, R., Loewen, G. R., Truglia, J. A., and Warrell, R. P., Jr. (1997) *J. Clin. Oncol.* **15,** 790–795
16. Wurtz, J. M., Bourguet, W., Renaud, J. P., Vivat, V., Chambon, P., Moras, D., and Gronemeyer, H. (1996) *Nat. Struct. Biol.* **3,** 87–94
17. Renaud, J. P., and Moras, D. (2000) *Cell. Mol. Life Sci.* **57,** 1748–1769
18. Nagy, L., Kao, H. Y., Love, J. D., Li, C., Banayo, E., Gooch, J. T., Krishna, V., Chatterjee, K., Evans, R. M., and Schwabe, J. W. (1999) *Genes Dev.* **13,** 3209–3216
19. Perissi, V., Staszewski, L. M., McInerney, E. M., Kurokawa, R., Krones, A., Rose, D. W., Lambert, M. H., Milburn, M. V., Glass, C. K., and Rosenfeld, M. G. (1999) *Genes Dev.* **13,** 3198–3208
20. Hu, X., and Lazar, M. A. (1999) *Nature* **402,** 93–96
21. Darimont, B., Wagner, R., Apriletti, J., Stallcup, M., Kushner, P., Baxter, J., Fletterick, R., and Yamamoto, K. (1998) *Genes Dev.* **12,** 3343–3356
22. Nolte, R. T., Wisely, G. B., Westin, S., Cobb, J. E., Lambert, M. H., Kurokawa, R., Rosenfeld, M. G., Willson, T. M., Glass, C. K., and Milburn, M. V. (1998) *Nature* **395,** 137–143
23. Brzozowski, A. M., Pike, A. C., Dauter, Z., Hubbard, R. E., Bonn, T., Engstrom, O., Ohman, L., Greene, G. L., Gustafsson, J. A., and Carlquist, M. (1997) *Nature* **389,** 753–758
24. Shiau, A. K., Barstad, D., Loria, P. M., Cheng, L., Kushner, P. J., Agard, D. A., and Greene, G. L. (1998) *Cell* **95,** 927–937
25. Pike, A. C., Brzozowski, A. M., Hubbard, R. E., Bonn, T., Thorsell, A. G., Engstrom, O., Ljunggren, J., Gustafsson, J. A., and Carlquist, M. (1999) *EMBO J.* **18,** 4608–4618
26. Bourguet, W., Ruff, M., Bonnier, D., Granger, F., Boeglin, M., Chambon, P., Moras, D., and Gronemeyer, H. (1995) *Protein Expression Purif.* **6,** 604–608
27. Gampe, R. T., Jr., Montana, V. G., Lambert, M. H., Wisely, G. B., Milburn, M. V., and Xu, H. E. (2000) *Genes Dev.* **14,** 2229–2241
28. Li, C., Schwabe, J., Banayo, E., and Evans, R. (1997) *Proc. Natl. Acad. Sci. U. S. A.* **94,** 2278–2283
29. Leslie, A. G. W. (1992) *CCP4 and ESF-EACMB Newsletter on Protein Crystallography,* No. 26, Daresbury Laboratory, Warrington, UK
30. CCP4 (1994) *Acta Crystallogr. Sect. D Biol. Crystallogr.* **50,** 760–763
31. Brunger, A. T., Adams, P. D., Clore, G. M., DeLano, W. L., Gros, P., Grosse-Kunstleve, R. W., Jiang, J. S., Kuszewski, J., Nilges, M., Pannu, N. S., Read, R. J., Rice, L. M., Simonson, T., and Warren, G. L. (1998) *Acta Crystallogr. Sect. D Biol. Crystallogr.* **54,** 905–921
32. Jones, T. A., Zou, J. Y., Cowan, S. W., and Kjeldgaard, M. (1991) *Acta Crystallogr. Sect. A* **47,** 110–119
33. Bourguet, W., Ruff, M., Chambon, P., Gronemeyer, H., and Moras, D. (1995) *Nature* **375,** 377–382
34. Peet, D. J., Doyle, D. F., Corey, D. R., and Mangelsdorf, D. J. (1998) *Chem. Biol.* **5,** 13–21
35. Kersten, S., Dawson, M., Lewis, B., and Noy, N. (1996) *Biochemistry* **35,** 3816–3824
36. Bourguet, W., Vivat, V., Wurtz, J. M., Chambon, P., Gronemeyer, H., and Moras, D. (2000) *Mol. Cell* **5,** 289–298
37. Gampe, R. T., Jr., Montana, V. G., Lambert, M. H., Miller, A. B., Bledsoe, R. K., Milburn, M. V., Kliewer, S. A., Willson, T. M., and Xu, H. E. (2000) *Mol. Cell* **5,** 545–555
38. Egea, P. F., Mitschler, A., Rochel, N., Ruff, M., Chambon, P., and Moras, D. (2000) *EMBO J.* **19,** 2592–2601
39. Chen, Z. P., Iyer, J., Bourguet, W., Held, P., Mioskowski, C., Lebeau, L., Noy, N., Chambon, P., and Gronemeyer, H. (1998) *J. Mol. Biol.* **275,** 55–65
40. Love, J. D., Gooch, J. T., Nagy, L., Chatterjee, V. K., and Schwabe, J. W. (2000) *Biochem. Soc. Trans.* **28,** 390–396
41. Canan Koch, S. S., Dardashti, L. J., Cesario, R. M., Croston, G. E., Boehm, M. F., Heyman, R. A., and Nadzan, A. M. (1999) *J. Med. Chem.* **42,** 742–750
42. Lala, D. S., Mukherjee, R., Schulman, I. G., Koch, S. S., Dardashti, L. J., Nadzan, A. M., Croston, G. E., Evans, R. M., and Heyman, R. A. (1996) *Nature* **383,** 450–453
43. Busch, K., Martin, B., Baniahmad, A., Martial, J. A., Renkawitz, R., and Muller, M. (2000) *Mol. Endocrinol.* **14,** 201–211
44. Lin, B. C., Hong, S. H., Krig, S., Yoh, S. M., and Privalsky, M. L. (1997) *Mol. Cell. Biol.* **17,** 6131–6138
45. Zhang, J., Hu, X., and Lazar, M. A. (1999) *Mol. Cell. Biol.* **19,** 6448–6457
46. Barroso, I., Gurnell, M., Crowley, V. E., Agostini, M., Schwabe, J. W., Soos, M. A., Maslen, G. L., Williams, T. D., Lewis, H., Schafer, A. J., Chatterjee, V. K., and O'Rahilly, S. (1999) *Nature* **402,** 880–883
47. Renaud, J. P., Rochel, N., Ruff, M., Vivat, V., Chambon, P., Gronemeyer, H., and Moras, D. (1995) *Nature* **378,** 681–689